

Submitted to the Editor of the ApJ Letters on June 30, 1998

## High-resolution Observations of OH(1720 MHz) Masers Toward the Galactic Center

F. Yusef-Zadeh

Department of Physics and Astronomy, Northwestern University, Evanston, IL 60208  
(zadeh@nwu.edu)

D. A. Roberts

NCSA, 405 N. Mathews Ave, Urbana, IL 61801 (dougr@ncsa.uiuc.edu)

W. M. Goss and D.A. Frail

National Radio Astronomy Observatory, P.O. Box 0, Socorro, New Mexico 87801  
(mgoss@aoc.nrao.edu), (dfrail@aoc.nrao.edu)

A. J. Green

University of Sydney, School of Physics, A28, Sydney, NSW 2006 Australia  
(agreen@physics.usyd.edu.au)

Received 00 1998;    accepted 00 1998

Re-submitted on August 15, 1998

## ABSTRACT

High-resolution VLA observations of 1720 MHz OH maser emission from Sgr A East and the circumnuclear disk with spatial and spectral resolutions of  $\approx 2''.5 \times 1''.3$  and  $0.27 \text{ km s}^{-1}$  are reported. This follow-up observational study focuses on the recent discovery of a number of such OH maser features and their intense circularly polarized maser lines detected toward these Galactic center sources. The 1720 MHz maser line of OH arises from collisionally excited gas behind a C-type shock and is an important diagnostic of the interaction process that may occur between molecular clouds and associated X-ray emitting shell-type supernova remnants. The present observations have confirmed that the observed Stokes  $V$  signal is due to Zeeman splitting and that the OH masers are angularly broadened by the scattering medium toward the Galactic center. The scale length of the magnetic field fluctuations in the scattering medium toward the Galactic center is estimated to be greater than 0.1-0.2 pc using the correlation of the position angles of the scatter-broadened maser spots. In addition, the kinematics of the maser spots associated with Sgr A East are used to place a 5 pc displacement between this extended radio structure and the Galactic center.

*Subject headings:* galaxies: ISM—Galaxy: center —ISM: individual (Sgr A East and Sgr A West) — ISM: magnetic fields

## 1. Introduction

A number of recent studies have shown OH(1720MHz) masers, when unaccompanied by the main transition lines at 1665 and 1667 MHz, are associated with molecular clouds interacting with expanding supernova remnants such as W28, W44, G359.1-0.5 (e.g. Frail, Goss & Slysh 1994; Yusef-Zadeh, Uchida, & Roberts 1995; Claussen et al. 1997). These observations support a model in which H<sub>2</sub> molecules, having kinetic temperature and density between 15-200 K and  $10^3 - 10^5 \text{ cm}^{-3}$ , respectively, collisionally pump OH molecules causing a population inversion in the 1720 MHz transition of OH molecules (Elitzur 1976). More recently, Wardle, Yusef-Zadeh, & Geballe (1998) suggest that water molecules produced behind a C-type shock must be dissociated by the X-ray flux from the SNR in order to enhance the abundance of the OH molecule.

The initial observations which reported the discovery of OH(1720MHz) maser lines toward Sgr A were carried out with a spectral resolution  $0.27 \text{ kms}^{-1}$  and a synthesized beam of approximately  $15''$  (Yusef-Zadeh *et al.* 1996, hereafter YRGFG). Seven OH(1720) masers were found to be associated with the nonthermal Sgr A East shell at a velocity of  $\approx 50 \text{ kms}^{-1}$ , which is close to the systemic velocity of the adjacent  $+50 \text{ kms}^{-1}$  cloud to the SNR. The eighth maser spot, however, showed a number of velocity components near  $134 \text{ kms}^{-1}$  at the location where the Northern Arm of Sgr A West crosses the circumnuclear disk (CND). In addition, the patterns of the Stokes *V* spectrum associated with the Sgr A East and the CND OH(1720MHz) maser spots were opposite to each other implying an opposite sign of the inferred magnetic field. We considered the OH(1720MHz) masers with two different kinematic and polarization characteristics in Sgr A are the result of two different events, namely the expansion of the nonthermal shell of Sgr A East inside the  $50 \text{ kms}^{-1}$  molecular cloud and cloud-cloud collisions with a relative velocity of  $134 \text{ kms}^{-1}$  in the CND (YRGFG).

Given the relatively low angular resolution of the previous observations, none of the sources were spatially resolved and it remained possible that the Zeeman effect could have been mimicked by two overlapping maser features with slightly different velocities and different polarization properties. The present observations with an order of magnitude more favorable spatial resolution compared to the earlier measurements show that in most cases the previous spectral features are heavily scatter-broadened and are indeed spatially separated from each other. In addition, the magnetic field strengths determined from Zeeman splitting of the maser spots are consistent with previous measurements.

## 2. Observations

The A configuration of the Very Large Array of the National Radio Astronomy Observatory<sup>1</sup> on November 22, 1996 was used to observe three fields centered on the B source ( $\alpha, \delta[1950] = 17^{\text{h}}42^{\text{m}}29^{\text{s}}.96, -28^{\circ}58'35''$  at  $V_{\text{LSR}}=134 \text{ km s}^{-1}$ ), the C source ( $17^{\text{h}}42^{\text{m}}28^{\text{s}}.07, -28^{\circ}58'32''.3$  at  $V_{\text{LSR}}=56 \text{ km s}^{-1}$ ), and the F source ( $17^{\text{h}}42^{\text{m}}32^{\text{s}}.6, -29^{\circ}00'23''.3$  at  $V_{\text{LSR}}=56 \text{ km s}^{-1}$ ) in the 1720 MHz hyperfine transition of OH molecule (YRGFC). Using both the right (*RCP*) and left (*LCP*) hands of circular polarization, the 195.3 kHz bandwidth and 127 channels gave a velocity resolution of  $0.27 \text{ km s}^{-1}$  after online Hanning smoothing. The final images had a synthesized beam of  $2''.48 \times 1''.28$  (PA= $3^{\circ}.9$ ) using the robustness parameter of 1 in IMAGR of AIPS with the exception of source B where using a robustness parameter of  $-5$  produces a spatial resolution of  $1''.6 \times 0''.82$  (PA= $-6^{\circ}.6$ ). The robustness parameter is used to apply different weighting to the *uv* data. Standard calibration was carried out using 1328+307 (flux density and bandpass) and

---

<sup>1</sup>The National Radio Astronomy Observatory is a facility of the National Science Foundation, operated under a cooperative agreement by Associated Universities, Inc.

1748-253 (complex gain and bandpass). The brightest isolated maser source A was used effectively to self-calibrate all the channels before the final cubes were constructed. The rms noise per channel is  $\approx 20$  and  $37 \text{ mJy beam}^{-1}$  for the low-resolution and high-resolution images, respectively. The analysis of the  $V$  signal due to the Zeeman effect followed the least-squares procedure of Roberts *et al.* (1993) in order to determine the line of sight magnetic field. The Stokes  $I$  and  $V$  spectra from the brightest maser A are shown in Figure 1. The solid line superposed on the  $V$  spectra is the derivative of the  $I$  spectra scaled by the derived magnetic field. The size of the sources were measured using the Gaussian-fitting algorithm JMFIT in AIPS on the channel that showed the peak emission. The errors were determined from the maximum and minimum values of the fit parameters that JMFIT gives. If these error parameters were zero, the errors could not be trusted and we did not incorporated them in our analysis. The flux density, LSR velocity, and velocity width were determined from Gaussian fits of the spectra using PROFIT in the Groningen Image Processing System (GIPSY). Table 1 lists the parameters of the fits to source B ( $v \approx 134 \text{ kms}^{-1}$ ) with a synthesized beam of  $1''.6 \times 0''.82$ , while Table 2 tabulates the parameters of the sources ( $v \approx 43\text{--}66 \text{ kms}^{-1}$ ) observed with a synthesized beam of  $2''.48 \times 1''.28$ . We have used the nomenclature introduced by YRGFG.

### 3. Results

#### 3.1. Sgr A West OH(1720MHz) Maser

The  $+134 \text{ kms}^{-1}$  velocity feature (B source in YRGFG) is spatially extended and shows a complex velocity structure resolved into four velocity components B1, B2, B3 and B4. The brightest sources B1 and B2 are partially blended spectrally but the positions of the peak emission are spatially coincident. Source B4 is displaced  $\approx 0.4''$  from B1 and B2 but shows a velocity similar to B1. The highest velocity feature at  $136.3 \text{ kms}^{-1}$  (source

B3) is displaced to the SW by about  $2''$  from the lower velocity components B1 and B2 at  $131.8$  and  $133.5 \text{ km s}^{-1}$  corresponding to a velocity gradient  $\approx 60 \text{ km s}^{-1} \text{ pc}^{-1}$ . This spatial distribution follows the N-S orientation of the ionized gas and the tongue of neutral cloud along the extension of the Northern Arm of Sgr A West (e.g. Jackson et al. 1993).

Sources B1 and B2 are clearly resolved with a size of  $0''.86 \pm 0.07 \times 0''.34 \pm 0.24$  with  $\text{PA} = 177^\circ \pm 6^\circ$ , and  $0''.63 \pm 0.24 \times 0''.44 \pm 0.17$  with  $\text{PA} = 168^\circ \pm 43^\circ$ , respectively. The axial ratio (minor/major) values of  $\approx 0.4$  and the position angles of all three sources in Table 1 are consistent to within the errors. The peak flux density of the B components is reduced by about 35% when compared with previous measurements using a more compact configurations of the VLA (YRGFG). It is quite possible that the observed change is due to a low surface brightness extended component resolved out by the present observation. Time variability over a ten month period is also a possibility that could contribute to the significant flux density variations. However, variability seems unlikely since all the components in Table 1 have lower intensities than the YRGFG results. The  $V$  spectrum of source B indicates a magnetic field strength of  $4.81 \pm 0.73 \text{ mG}$ . This value is the largest magnetic field yet estimated in the Galactic center region from OH Zeeman data. Because of the relatively large Zeeman shift of the line profiles observed with respect to their Doppler linewidths, Elitzur (1998) has recently argued that the Galactic center OH(1720MHz) maser lines reported by YRGFG are saturated. We have used his novel approach to determine if the present data show any signatures of maser saturation. Sources A, C, D and E all show signatures of saturated masers with the value of the quantity  $\tau_0$  ranging between 28 and 81 (see equation 32 of Elitzur 1998 where  $\tau_0$  is defined as  $T_b = T_x e^{\tau_0}$  and  $T_b$  and  $T_x$  are the maser brightness and excitation temperatures, respectively).

### 3.2. Sgr A East OH(1720MHz) Masers

The seven sources detected by YRGFG are summarized in Table 2. Two additional components (H & I) are detected in the A array observations. The brightness temperature of the strongest source A (size  $0''.74 \pm 0''.025 \times 0''.55 \pm 0''.025$ ) is  $\approx 8.1 \times 10^5$  K implying that the OH (1720MHz) emission is produced under non-thermal conditions. The axial ratios of the sources with the most favorable signal to noises (A, D, E and G1 in Table 2) are in the range 0.72 to 0.81. The position angle of their semi-major axis vary significantly between sources A and the remainder of the resolved sources. We also note that the sources surrounding the non-thermal shell of Sgr A East, as discussed below, show two distinct velocity components. The maser features located to the SW of the shell have velocities ranging between 53 and 66  $\text{kms}^{-1}$  whereas source C to the NW of the shell has a velocity of 43  $\text{kms}^{-1}$ .

## 4. Discussion

### 4.1. The Nature of Scattering

Recent observations show that the interstellar broadening of Sgr A\* and of OH/IR stars within the inner 45' of the Galactic center is anisotropic (Lo *et al.* 1993; van Langevelde *et al.* 1992; Yusef-Zadeh *et al.* 1994; Frail *et al.* 1994; Lazio and Cordes 1998). The scatter-broadened image of Sgr A\* is elongated in the East-West direction, with an axial ratio of  $0.60 \pm 0.05$  at  $\lambda 20$  cm and a position angle of  $87^\circ \pm 3^\circ$ . Both the major and minor axes follow the  $\lambda^2$  law appropriate for scattering by turbulence in the intervening medium. The size of the heavily anisotropically scattered OH/IR stars at 1612 MHz based on A-array observations ranges between  $0''.5$  and  $1''.5$  (Frail *et al.* 1994). The anisotropy is considered to be caused by a magnetic field permeating the scattering medium (e.g. van Langevelde

et al. 1992), and that the scattering is agreed to occur within extended HII regions lying in the central 100 pc of the Galaxy (Yusef-Zadeh et al. 1994).

Assuming that sources A to I are single sources and that their sizes are not intrinsic, the measured sizes agree very well with the heavily scattered radio OH/IR stars in the Galactic center region (Frail et al. 1994). Source C, however, is unresolved suggesting that the scattering medium is inhomogeneous. The sources listed in Tables 1 and 2 also show a degree of anisotropy with the Sgr A West B sources having typical axial ratio of  $\approx 0.4$  but somewhat less than the values of  $\approx 0.7$  for the Sgr A East maser sources. It is known that Sgr A East lies behind Sgr A West (Yusef-Zadeh and Morris 1987; Pedlar et al. 1989). Thus the larger degree of anisotropy for the B sources may indicate averaging of the sources over a larger pathlength (see below). We also note a trend in the position angle distribution of the scattered sources. The clusters of resolved sources in close proximity appear to show similar position angles, whereas the sources that are more displaced show no apparent correlation in their position angles. Figure 2 shows a  $\lambda 6\text{cm}$  continuum image of Sgr A East and Sgr A West with a resolution of  $0.67'' \times 0.40''$  (PA= $7^\circ$ ). The shapes of the resolved sources in Tables 1 and 2 are drawn on Figure 2 (the actual sizes are 15 times smaller than those drawn). Two other heavily scattered sources are also drawn, namely Sgr A\* and OH359.986–0.061 (1612 MHz) as discussed below.

The variation of the position angle of scatter broadened radio sources can be used as a powerful probe of the structure of the ionized magnetized medium toward the Galactic center. Using Sgr A\* with a position angle of  $82^\circ \pm 1.8$  at  $\lambda = 20.7\text{cm}$  (Yusef-Zadeh et al. 1996) and the Sgr A West sources (sources B1, B2 and B4 in Table 1) with similar position angles (in the range 177 and 23 degrees, see Figure 2) we can examine the spatial scale of the magnetic fluctuations. The position angles of the B sources and Sgr A\*, separated by about  $45''$  ( $\approx 1.8$  pc at the distance of 8.5 kpc), show no correlation whereas the B



sources that are separated by  $\approx 3''$  show a reasonable correlation. This implies that the thickness of the magnetoionized screen must be between  $3''$  and  $45''$ . If the thickness of the screen, assumed to be near the Galactic center, is much larger than the spatial scale  $0.1$  pc, averaging along the line of sight would substantially reduce the correlation of the orientation of the scattered sources. This picture is also consistent with the lack of correlation between the position angles of Sgr A\* and the nearest OH/IR star (OH359.986-0.061) is shown as the ellipse to the NE in Figure 2 (Frail et al. 1994). This star lies about  $160''$  from Sgr A\* corresponding to a projected linear separation of  $\approx 6$  pc, much larger than the estimated scale length of the magnetic fluctuations.

The above interpretation based on limited number of scattered sources can also be applied to the OH(1720MHz) masers associated with Sgr A East. While sources D and E, separated by  $\approx 4''$  show position angles that agree with each other ( $29^\circ, 48^\circ$ ) within the errors, source A and to some extent source G1 show discrepant position angles of  $147^\circ$  and  $4.5^\circ$ , respectively. Sources A and G1 are displaced by more than  $20''$  ( $0.8$ pc) from sources D and E. The lack of correlation suggests a scale length of magnetic fluctuations greater than  $0.1$  pc (the distance between sources D and E) and less than  $0.8$  pc.

It is evident from the above analysis that the power in the smallest length scale in the turbulent medium with a thickness of greater than about  $0.1$  pc varies considerably. Recent analysis of the rotation measure structure function of the Faraday screen toward the non-thermal filamentary structure G359.54+0.18 suggests a thickness which is about  $0.1$  pc (Yusef-Zadeh, Wardle, & Parastaran 1997). In this picture the variation of the rotation measure on scales of about  $0.1$  pc was used to estimate the thickness of the magnetoionized medium. With the limited number of maser sources available as a function of angular separations, it is striking that the scale length of the magnetic fluctuations for the regions of Sgr A and G359.5+0.18 based on two different measurements are similar.

## 4.2. Tidal Shear in Sgr A East

The maser sources arise along the edge of the Sgr A East shell where the acceleration is considered to be perpendicular to the line of sight and where the velocity coherence is achieved with a small velocity gradient along the line of sight. This picture is consistent with the morphology of  $\text{NH}_3$  and CS molecular features thought to be the result of the compression of the  $50 \text{ km s}^{-1}$  molecular cloud as the shock is driven into the cloud (Ho et al. 1991; Serabyn et al. 1992). The maser sources detected to the SE of Sgr A East lie close to the elongated compressed CS feature. Earlier measurements of Galactic SNR’s interacting with molecular clouds showed a similarity between radial velocities of the OH(1720MHz) masers distributed at the edge of the remnants and the systemic velocities of the disturbed molecular clouds (Frail et al. 1996; Green et al. 1997). It is plausible that the large velocity difference of masers seen in Sgr A East may be the result of a strong tidal shear that the  $50 \text{ km s}^{-1}$  molecular cloud is experiencing. The velocity gradient of maser sources across the SE and NW edges of the Sgr A East shell is estimated to be  $\approx 2 \text{ km s}^{-1} \text{ pc}^{-1}$ . The average velocity difference between sources C and A-G is  $\Delta V = 12 \text{ km s}^{-1}$  with a linear separation of  $\approx 6 \text{ pc}$ . Assuming a mass distribution  $M(r) \propto r^{1.2}$  (e.g. Morris and Serabyn 1997; Mezger 1997), the above parameters suggest that Sgr A East has to be located to within 5 pc behind the Galactic center (Yusef-Zadeh and Morris 1987; Pedlar et al. 1989).

In summary, we have reported high resolution observations of OH(1720) MHz masers associated with a nonthermal radio source (Sgr A East) and the thermal source (Sgr A West), both of which are interacting with their corresponding molecular clouds. The study of the OH(1720MHz) masers in the Galactic center region have provided us with important physical quantities such as the line of sight magnetic field behind a shock front, the size and shape of scatter-broadened sources masked by the turbulent screen toward the Galactic center, the length scale of the magnetic fluctuations in the scattering medium and the

magnitude of the tidal shear experienced by an expanding nonthermal shell into a dense molecular cloud.

## REFERENCES

- Claussen, M.J., Frail, D.A., Goss, W.M., & Gaume, R.A. 1997, ApJ 489, 143.
- Elitzur, M. 1976, ApJ, 203, 124
- Elitzur, M. 1998, ApJ, in press.
- Frail, D.A., Diamond, P.J., Cordes, J.M. and van Langevelde, H.J. 1994, ApJ, 427, L43
- Frail, D. A., Goss, W. M., Reynoso, E. M., Green, A. J. & Otrupcek, R. 1996, AJ, 111, 1651
- Frail, D.A., Goss, M.W. and Slysh, V.I. 1994, ApJ, 424, L111
- Green A.J., Frail, D.A., Goss, W.M. & Otrupcek, R. 1997, AJ, 114, 2058.
- Ho, P.T.P., Ho, L.C., Szczepaniski, J.C. Jackson, J.M., Armstrong, J.T. & Barrett, A.H. 1991, Nature, 350, 309.
- Jackson, J.M., Geis, N., Genzel, R., Harris, A.I., Madden, S., Poglitsch, A., Stacey, G.J., Townes, C.H. 1993, ApJ 402, 173.
- Lazio, T.J. & Cordes, J. ApJS, in press.
- Lo, K.Y., Backer, D.C., Kellermann, K.I., Reid, M., Zhao, J.H. *et al.* , 1993, Nature, 362, 38.
- Mezger, P.G. 1997, IAUS 184, 168.
- Morris, M. & Serabyn, G. 1997, ARA&A 34, 645.
- Pedlar, A., Anantharamaiah, K.R., Ekers, R.D., Goss, W.M., van Gorkom, J.H., Schwarz, U.J., & Zhao, J.-H. 1989, ApJ 342, 769.
- Roberts, D.A., Goss, W.M. 1993, ApJS, 86, 133
- Serabyn, E., Lacy, J.H., & Achtermann, J.M. 1992, ApJ, 395, 166.
- van Langevelde, H.J., Frail, D.A., Cordes, J.M., & Diamond, P.J. 1992, ApJ, 396, 686

Wardle, M., Yusef-Zadeh, F., & Geballe 1998, submitted to ApJ.

Yusef-Zadeh, F., Cotton, W., Wardle, M., Melia, F. & Roberts, D.A. 1994, ApJ, 434, L63.

Yusef-Zadeh, F., Uchida, K.I., & Roberts, D.A. 1995, Science 270, 1801.

Yusef-Zadeh, F., Roberts, D.A., Goss, W.M., Frail, D. & Green, A. 1996, ApJ 466, L25 (YRGFG).

Yusef-Zadeh, F., Wardle, M., & Parastaran, P. 1997, ApJ 475, L119.

Yusef-Zadeh, F. & Morris, M. 1987, ApJ, 320, 545.

F. Yusef-Zadeh’s work was supported in part by NASA grant NAGW-2518. D. Roberts acknowledges support from NSF grant AST94-19227. We thank Mark Wardle and Mark Claussen for useful discussion.

---

This manuscript was prepared with the AAS L<sup>A</sup>T<sub>E</sub>X macros v4.0.

Fig. 1.— The Stokes  $I$  and  $V$  spectra from the most intense maser A in Sgr A East. The solid line superposed on the  $V$  spectra is the derivative of the respective  $I$  spectra scaled by the derived line of sight magnetic field ( $3.68 \pm 0.12$ ) due to Zeeman splitting.

Fig. 2.— A  $\lambda 6\text{cm}$  continuum image of the shell-like nonthermal source Sgr A East and a spiral-like Sgr A West (saturated) with a resolution of  $0.67'' \times 0.40''$  (PA= $7^\circ$ ). The shapes of the resolved sources in Tables 1 and 2 are drawn but the sizes are drawn 15 times bigger than the actual values. Two other heavily scattered sources are also indicated, Sgr A\* close to the center of Sgr A West and OH359.986–0.061 to the northwest of the Sgr A East shell.

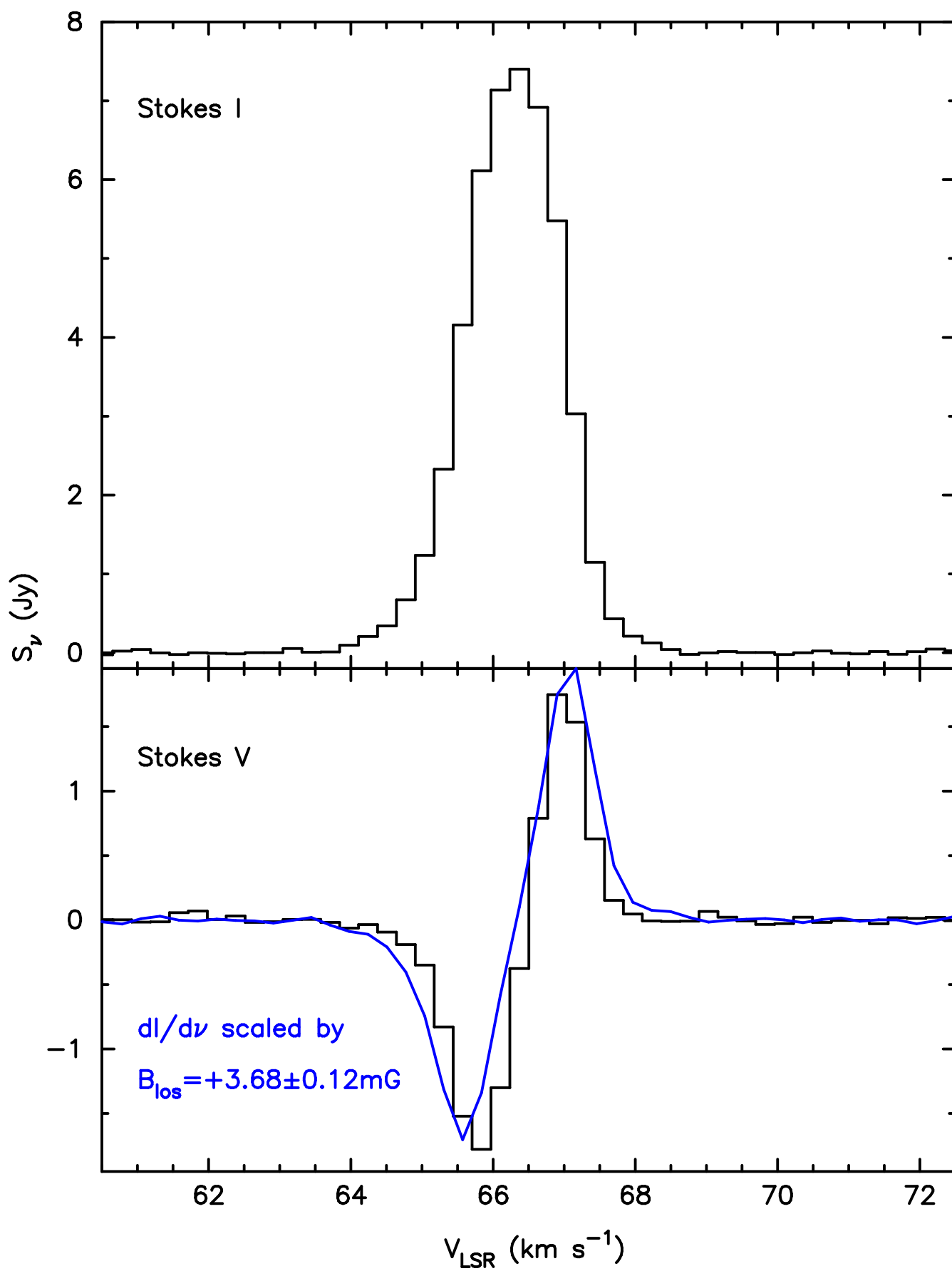


TABLE 1  
GAUSSIAN FITS FOR OH(1720 MHz) MASER FEATURES: B SOURCES

Maser Designation	$\alpha_{1950}$ (h m s)	$\delta_{1950}$ ( $^{\circ}$ ' ")	$S_p$ (Jy)	$V_{\text{LSR}}$ (km s $^{-1}$ )	$\Delta V$ (km s $^{-1}$ )	$B_{\text{los}}$ (mG)	Size		PA	axial ratio
							major	minor		
Sgr A OH1720:B1 (132)	17 42 29.92	−28 58 34.6	0.68±0.14	+131.8±0.06	1.32±0.01	−4.48±0.46	0.86±0.07	0.34±0.05	177±6	0.39±0.06
Sgr A OH1720:B2 (134)	17 42 29.92	−28 58 34.6	0.74±0.11	+133.5±0.11	2.20±0.20	−4.48±0.46	0.63±0.24	0.44±0.17	168±43	0.7±0.38
Sgr A OH1720:B3 (136)	17 42 29.98	−28 58 36.7	0.35±0.04	+136.3±0.04	1.34±0.10	−4.81±0.73	—	—	—	—
Sgr A OH1720:B4 (132)	17 42 29.85	−28 58 34.7	0.54±0.05	+131.6±0.04	1.40±0.09	−2.80±0.37	0.94±0.09	0.36±0.15	23±8	0.4±0.2



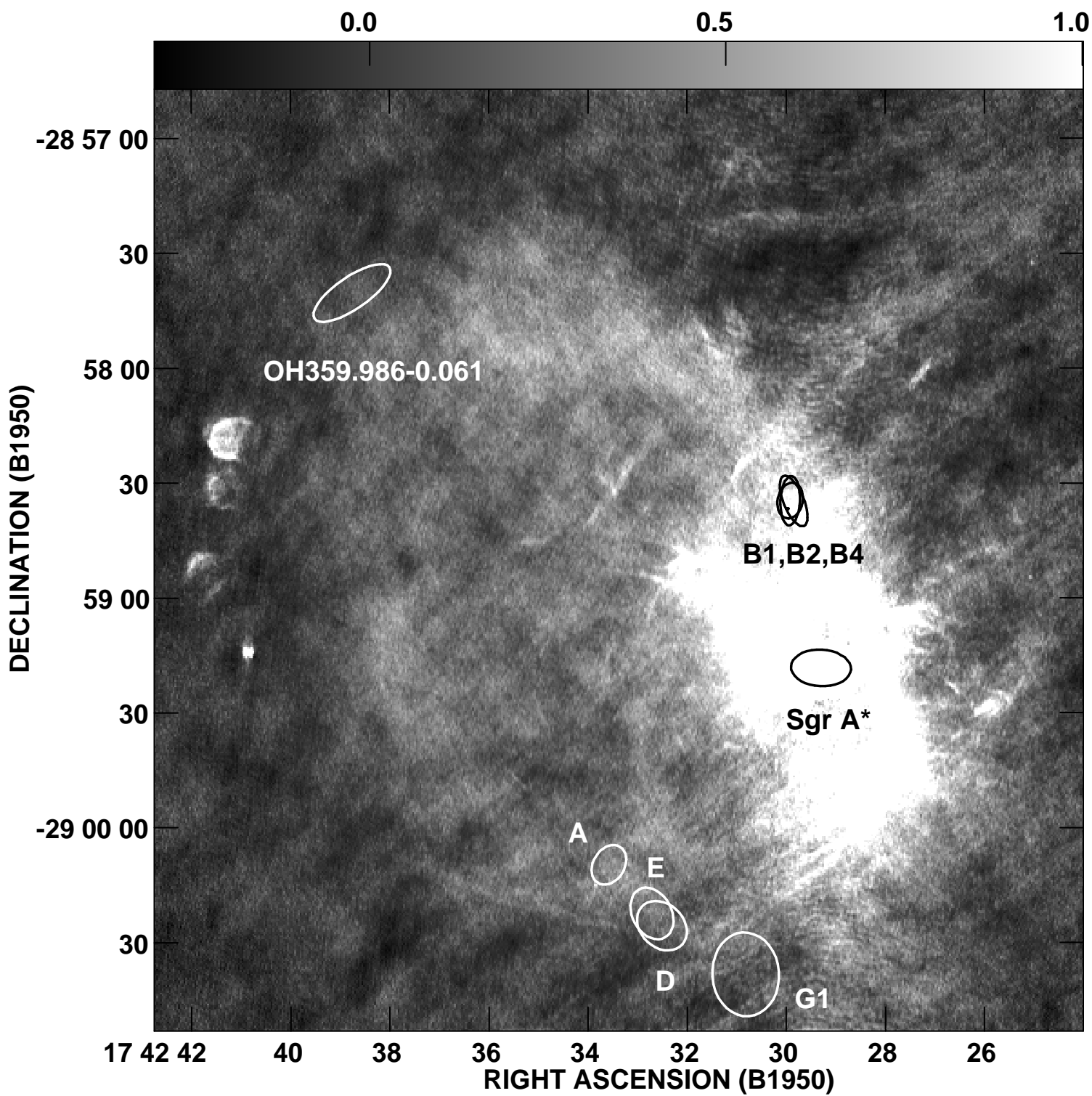


TABLE 2  
GAUSSIAN FITS FOR OH(1720 MHz) MASER FEATURES

Maser Designation	$\alpha_{1950}$ (h m s)	$\delta_{1950}$ ( $^{\circ}$ ' ")	$S_p$ (Jy)	$V_{LSR}$ (km s $^{-1}$ )	$\Delta V$ (km s $^{-1}$ )	$B_{los}$ (mG)	Size			axial ratio
							major	minor	PA	
Sgr A OH1720:A (66)	17 42 33.58	−29 00 09.7	7.37±0.07	+66.25±0.01	1.55±0.01	+3.68±0.12	0.74±0.03	0.55±0.03	148±5	0.74±0.05
Sgr A OH1720:C (43)	17 42 28.10	−28 58 33.0	0.76±0.03	+43.27±0.01	0.95±0.03	+3.11±0.21	—	—	—	—
Sgr A OH1720:D (53)	17 42 32.51	−29 00 25.6	0.58±0.03	+52.67±0.02	0.99±0.03	+2.80±0.30	0.97±0.20	0.76±0.28	48±40	0.78±0.33
Sgr A OH1720:E (56)	17 42 32.71	−29 00 22.4	0.79±0.03	+57.40±0.02	1.25±0.03	+2.32±0.23	0.95±0.15	0.69±0.13	29±24	0.72±0.18
Sgr A OH1720:F (62)	17 42 32.53	−29 00 23.3	0.23±0.02	+62.10±0.04	1.32±0.1	(3.6) <sup>a</sup>	—	—	—	—
Sgr A OH1720:G1 (54)	17 42 30.82	−29 00 38.3	0.34±0.06	+54.26±0.03	1.11±0.11	+2.50±0.46	1.46±0.26	1.18±0.17	5±38	0.81±0.18
Sgr A OH1720:G2 (56)	17 42 30.83	−29 00 37.8	0.12±0.03	+55.52±0.32	3.30±0.45	+2.50±0.46	—	—	—	—
Sgr A OH1720:H (49)	17 42 32.07	−29 00 32.7	0.15±0.03	+49.25±0.05	0.69±0.11	+1.84±0.55	—	—	—	—
Sgr A OH1720:I (58)	17 42 32.24	−29 00 26.7	0.16±0.03	+58.37±0.04	0.60±0.09	(2.7) <sup>a</sup>	—	—	—	—

<sup>a</sup>3  $\sigma$  upper limit.